Chinese Chemical Letters 37 (2026) 112229

Contents lists available at ScienceDirect

Chinese Chemical Letters

journal homepage: www.elsevier.com/locate/cclet

Surface functionalization of polyaniline *via* click reaction for the preparation of luminescent conductive materials

Xiangrong Xu[a], Lifeng Zhang[b], Ming Zhang[a], Yiyang Zhang[a,*], Lei Yu[a,*]

[a] School of Chemistry and Materials, Yangzhou University, Yangzhou 225002, China
[b] Department of Electrical and Electronic Engineering, Kyushu Institute of Technology, Kitakyushu 8048550, Japan

ARTICLE INFO

Article history:
Received 27 August 2025
Revised 21 November 2025
Accepted 7 December 2025
Available online 8 December 2025

Keywords:
Polyaniline
Fluorescence
Click chemistry
Conductivity
9-Anthracene formyl chloride

ABSTRACT

The emissive layer of stretchable optoelectronic devices currently incorporates luminescent units through physical blending or co-polymerization. However, these methods often compromise material performance due to interference from the introduced functional groups, and a significant portion of the luminescent components embedded within the material is wasted. In this work, we propose an innovative "click chemistry" strategy for integrating luminescent functional groups onto the surface of polyaniline (PANI) through a simple stirring process. After proton doping, the functionalized PANI exhibited a 29-fold increase in electrical conductivity compared to pristine PANI. This improvement originates from the extended conjugation of the anthracene moiety and enhanced proton-doping efficiency, making it promising for advanced electronic devices.

© 2026 Published by Elsevier B.V. on behalf of Chinese Chemical Society and Institute of Materia Medica, Chinese Academy of Medical Sciences.

Polyaniline (PANI) is widely recognized as one of the most prominent conductive polymers [1–3]. In addition to its high electrical conductivity, excellent film-forming properties [4], and remarkable chemical stability [5], the conjugate units in the polyaniline structure also contribute to its photoluminescent properties [6]. As a result, polyaniline can be utilized in the fabrication of electroluminescent devices [7], sensors [8], and other applications [9–11]. However, the photoluminescent performance of polyaniline under ultraviolet excitation is relatively weak. Therefore, enhancing the fluorescence intensity of polyaniline *versus* specific wavelength light by incorporating luminescent functional groups has become a significant research focus. Currently, the conventional approach to preparing fluorescent polymers primarily involves designing fluorescent monomers first and then polymerizing these monomers into polymers [12,13]. However, this method presents two major drawbacks: Firstly, the introduced groups on the monomers can interfere the polymerization process, compromising the mechanical properties of the synthesized material. For PANI synthesis, the introduced groups on aniline may disturb the oxidative polymerization process and result in the poor yield of PANI [14]. Secondly, the polymerization process can lead to many fluorescent groups being embedded within the material, preventing them from fully exhibiting their fluorescent properties. This not only results in the wastage of fluorescent components but also raises concerns due to the relatively high cost and tedious procedures for preparing such monomers. Additionally, according to existing literature, fluorescent polyaniline can also be synthesized through chemical reactions between polyaniline and fluorescent compounds [15–17]. Nevertheless, this synthesis process requires electrochemical polymerization, catalysts, and extended reaction times, which increase the reaction cost and reduce efficiency. Although fluorescent conductive materials can be fabricated by blending PANI with luminescent materials, the introduced luminescent components may interfere with the intermolecular interactions of PANI, leading to decreased electrical conductivity.

Yet, click chemistry refers to a set of powerful and nearly 100% reliable selective reactions that enable the efficient and straightforward generation of molecular diversity by establishing new combinatorial chemistry methods based on carbon-heteroatom bond (C-X-C) formation [18]. It has been reported that click reactions are characterized by fast reaction rates, high reactivity, excellent selectivity, mild conditions, and minimal byproducts, making them widely applicable in numerous fields such as biomedicine and materials science [19–23]. Consequently, C. R. Bertozzi, K. B. Sharpless and M. Meldal were awarded the 2022 Nobel Prize in Chemistry for their contributions to this field. To date, click reactions that have been employed in the preparation of fluorescent materials including B-O formation [24], amino–yne reaction [25], azide-alkyne reaction [26], photoinduced defluorinative acyl fluoride exchange [27], thiol–yne reaction [28], thiol-ene reaction [29], and

* Corresponding authors.
E-mail addresses: 008011@yzu.edu.cn (Y. Zhang), yulei@yzu.edu.cn (L. Yu).

https://doi.org/10.1016/j.cclet.2025.112229
1001-8417/© 2026 Published by Elsevier B.V. on behalf of Chinese Chemical Society and Institute of Materia Medica, Chinese Academy of Medical Sciences.

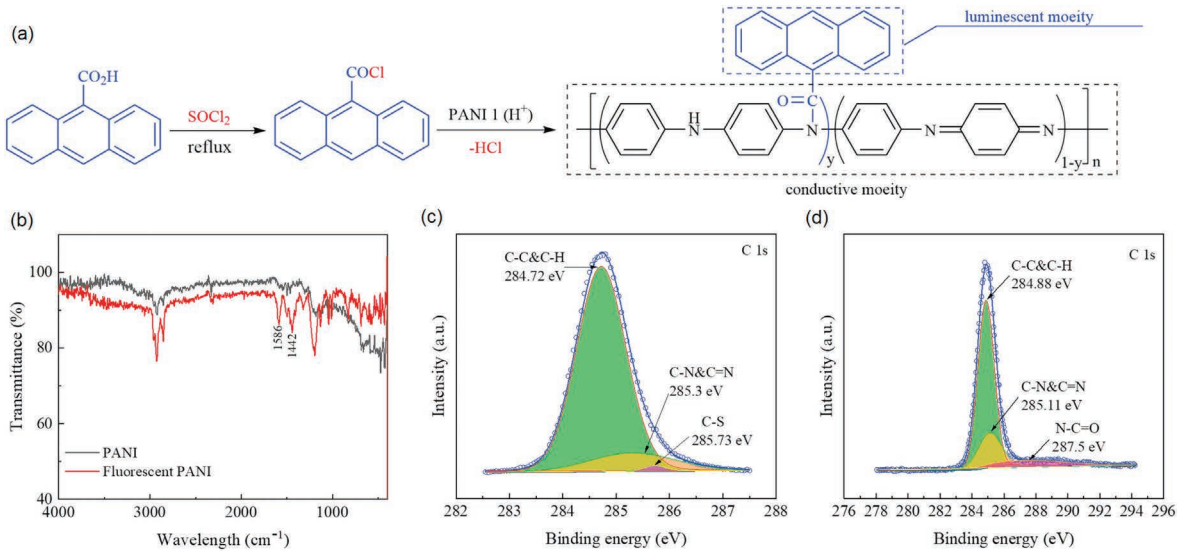


Fig. 1. Synthesis and the characterizations. (a) Synthesis of fluorescent PANI. (b) FT-IR spectra of PANI (black) and fluorescent PANI (red). (c) XPS spectrum of PANI. (d) XPS spectrum of fluorescent PANI.

tetrazole-alkene reaction [30]. However, the application of click reactions between acyl chloride and amino groups in fluorescent materials, as well as their use in the synthesis of fluorescent materials based on PANIs, has rarely been reported. Driven by the requirements of related projects and inspired by recent literatures [31–33], we proposed a novel approach to synthesize the fluorescent PANI first using the click chemistry strategy, and then uploaded the fluorescent group into the material by immersing it with anthracene formyl chloride. The fluorescent anthracene group could be firmly attached to the PANI chain through amide bond. It was found that the fluorescence of the treated PANI is significantly enhanced at specific wavelengths, while its conductivity could be enhanced. Herein, we report our findings.

PANI was initially synthesized *via* traditional method, while the luminescent reagent anthracene-9-carboxylic acid was treated by $SOCl_2$ to prepare the active 9-anthracene formyl chloride. The reaction of the colloidal suspension of PANI **1** (H^+) with 9-anthracene formyl chloride in CH_2Cl_2 occurred rapidly and give the fluorescent PANI **2** solution. After evaporating the solvent, the residue was washed with aqueous Na_2CO_3 and deionized water respectively to give the fluorescent PANI material **2**. In the material, anthracene is the luminescent moiety (blue) while PANI chain is the conductive moiety (black), and they are linked by the amide bond (Fig. 1a).

Fig. 1b presents the Fourier transform infrared spectra of polyaniline before and after functionalization with the fluorescent group. In the spectrum of **2**, the strong absorption peak at 1442 cm^{-1}, corresponding to the C=C stretching vibration, confirms the successful incorporation of the anthryl group. The peak at 1586 cm^{-1}, attributed to the carbonyl group of the amide bond linking the fluorescent group to the polyaniline chain, exhibits a red shift compared to the typical amide carbonyl absorption range (1620–1670 cm^{-1}). This shift is likely caused by hydrogen bonding interactions between the fluorescent polyaniline chains.

X-ray photoelectron spectroscopy (XPS) analysis of the materials was performed to verify the change of the chemical environments at molecular level. The C 1s peak fitting results of **1** (H^+) and **2** are shown in Figs. 1c and d, respectively. In the spectrum of **1** (H^+), carbon exists in three bonding states: the peak at a binding energy of 284.72 eV corresponds to C–C and C–H bonds, the peak at 285.3 eV corresponds to C–N and C=N bonds, and the peak at 285.73 eV corresponds to C-S bonds. For the material **2**, carbon still exists in these three bonding states, but the binding energies have

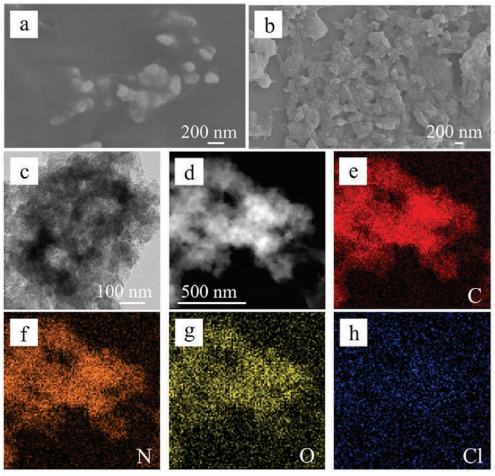


Fig. 2. Morphology characterizations. (a) SEM image of **1** (H^+). (b) SEM image of **2**. (c) HRTEM image of **2**. (d) HAADF-STEM image of **2**. (e-h) EDS elemental mappings of C, N, O and Cl in **2**.

shifted to 284.88, 285.11, and 287.5 eV, respectively. This indicates that the introduction of the fluorescent group significantly affects the chemical environment of carbon in the material. By comparing Fig. 1c with d, it can be observed that the peak area of C–C and C–H bonds in **2** has decreased, suggesting that the subsequent washing process of removing excess anthracene-9-carboxylic acid and 9-anthracene formyl chloride also elutes the doped anions. Additionally, in the XPS spectrum of **2**, the signals of C–N and C=N bonds are significantly enhanced, indicating that the click reaction between acyl chloride and polyaniline has formed more C–N bonds. The C–S peak in the XPS spectrum of **1** (H^+) originates from dodecylbenzenesulfonic acid (DBSA) dopants (Fig. 1c). After alkaline washing, in compound **2**, DBSA could be removed and related peak disappeared (Fig. 1d).

To understand the morphological changes of the samples before and after introducing anthracene groups, scanning electron microscopy (SEM) was used to characterize **1** (H^+) and **2**. The SEM images are shown in Figs. 2a and b. It can be seen from the figures that the particles of **1** (H^+) and **2** are basically spherical and their particle sizes are <100 nm, indicating that the click reaction

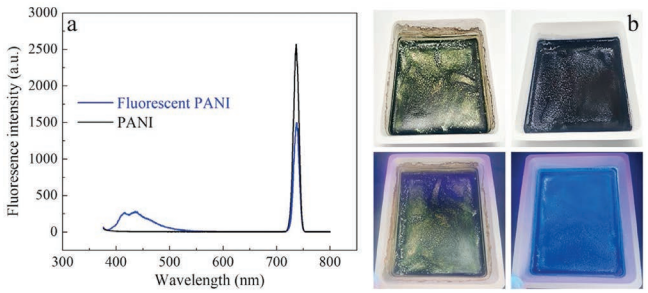


Fig. 3. Fluorescence properties of the materials. (a) Emission spectra of **1** (H^+) and **2** under excitation with 366 nm wavelength light. (b) Photographs of **1** (H^+) (left) and f **2** (right) under white light (upper) and 365 nm wavelength ultraviolet light (lower).

Table 1
The electrical conductivity (C) of the materials.

Entry	Samples	C (S/cm)[c]
1	**1**	≈ 0
2	**1** (H^+)[a]	7.847×10^{-3}
3	**1** + fluorescer[b]	≈ 0
4	**1** (H^+) + fluorescer	5.253×10^{-5}
5	**2**	≈ 0
6	**2** (H^+)[a]	0.232
7	**3** (H^+)[d]	5.380×10^{-2}

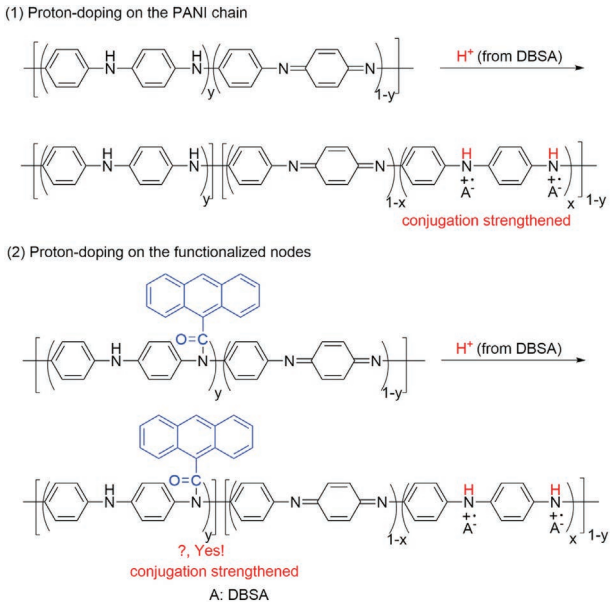
[a] "(H^+)" means chemically synthesized polyaniline being doped with protons.
[b] Mechanical mixture with 5 % of anthracene-9-carboxylic acid (fluorescer).
[c] For experimental details, please see Supporting information.
[d] PANI **3** was synthesized *via* the method similar to **2** but with benzoyl chloride as the functionalization reagent.

did not significantly change the particle size of polyaniline. The agglomeration phenomenon of the materials may be caused by the hydrogen bond interaction between molecular chains.

To further observe the morphology of **2** and overcome the adverse effects of agglomeration on its morphological observation, transmission electron microscopy (TEM) was then employed. As shown in Fig. 2c, the material is formed by a lot of nano-scale microspheres with their particle sizes <100 nm. The high-angle annular dark field scanning transmission electron microscope (HAADF-STEM) image of **2** and the corresponding elemental distribution maps are shown in Figs. 2d–g, where C, N, and O, are uniformly dispersed, suggesting homogeneous surface modification. The Cl element (Fig. 2h) is likely incorporated from HCl, which is the by-product of the reaction of chloride.

The click reaction of **1** (H^+) occurred quickly and only 20 s reaction time was enough to prepare **2** (Fig. S1 in Supporting information). The fluorescence spectra of **1** (H^+) (black) and **2** (blue) are shown in Fig. 3a. Upon excitation at 366 nm, a weak overtone peak at ~730 nm was observed for compound **2**, rather than a fluorescence signal. The introduction of anthracene groups enhanced fluorescence at 400–500 nm, confirming successful surface functionalization. Photographs of the materials are in accordance with the emission spectra, as shown in Fig. 3b, blue fluorescence (right, lower) can be clearly observed when lightening **2** with the 366 nm wavelength light. The fluorescence enhancement phenomenon can also be described by Fig. S2 (Supporting information).

The conductivity of the materials can be determined *via* the four-probe method (Fig. S3 in Supporting information). The de-doped state material **1** does not exhibit conductivity (Table 1, entry 1). Comparatively, the doped material **1** (H^+) is a conductive polymer, with its conductivity determined to be 7.847×10^{-3} S/cm (Table 1, entry 2). After treating PANI **1** (H^+) with alkaline solution, the doped state PANI **1** (H^+) could be converted into its de-doped state PANI **1**. The deprotonation of PANI chain leads to the disappearance of ammonium ions, which weaken the conjugation system formed by the p-π conjugation. Thus, the conjugation skeleton is reduced, resulting in the electrical conductivity of the material (Table 1 entries 2 *vs.* 1) [34].



Scheme 1. Proton-doping of PANIs to improve their electrical conductivity.

The fluorescence can also be imparted to the material by mechanically incorporating fluorescent molecules into it. However, although the fluorescent agent anthracene-9-carboxylic acid is a carboxylic acid, its mechanical mixture with polyaniline **1** does not exhibit conductivity (Table 1, entry 3). After mechanically blending PANI **1** (H^+) with a fluorescent agent anthracene-9-carboxylic acid, the conductivity of the mixture is improved, but is still lower than that of the PANI **1** (H^+) (Table 1, entries 4 *vs.* 2). This is because the fluorescent molecules incorporated by mechanical doping will interrupt the interactions between the conductive molecular chains of polyaniline, thereby reducing its electrical conductivity. Comparatively, the functionalized PANI **2** exhibits excellent electrical conductivity. Although the de-doped state **2** does not exhibit conductivity (Table 1, entry 5), the doped state PANI **2** (H^+) is an excellent conductor (Table 1, entry 6). Its conductivity was determined to be 0.232 S/cm, *i.e.*, >29 times higher than the doped state PANI **1** (H^+) (Table 1, entries 6 *vs.* 2). As shown in Scheme 1, introducing 9-anthracene formyl onto PANI chain could expand the conjugated system, resulting in the improved electrical conductivity of the functionalized materials. This improvement originates from the extended conjugation of the anthracene moiety and enhanced proton-doping efficiency, in addition to avoiding luminescent waste.

From a molecular perspective, the functionalization of PANI with acyl chlorides may lead to a decrease in electrical conductivity. This is because the formed amides are generally difficult to be protonated, which turns them into "breakpoints" in the conjugated conductive system and thus weakens the material's conductivity. However, Table 1 shows the opposite result. This is because the reagent used for functionalization is 9-anthracene formyl chloride. The anthracene ring has a high electron cloud density, which reduces the weakening effect of the acyl group on the electron cloud density of nitrogen, making the formed amide possibly protonated. To prove this hypothesis, we synthesized similar PANI material **3** by using benzoyl chloride as the functionalization reagent. The electrical conductivity of doped **3** (H^+) was determined to 5.380×10^{-2} S/cm, obviously lower than that of **2** (H^+) as expected (Table 1, entry 7).

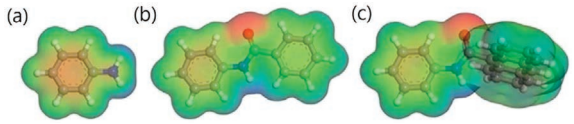


Fig. 4. Calculation of the electron cloud density of the nitrogen atoms.

Additionally, the electron cloud density maps of three molecules were drawn using Materials Studio software, as shown in Fig. 4. In the molecule of aniline, the aryl ring and nitrogen atom are the regions with relatively high electron cloud density (Fig. 4a). After amidation reactions with benzoyl chloride and 9-anthracenecarbonyl chloride, the electron cloud densities of the nitrogen atoms and the benzene rings decreased as expected (Figs. 4a and b). Due to the electron-donating effect of the aromatic rings, the electron cloud density on the amide nitrogen atom can still support the occurrence of protonation reactions, thereby avoiding the destruction of the p-π conjugated system. Instead, the introduction of the aromatic rings enlarges the conjugated system, leading to an increase in the electrical conductivity of the materials (Table 1, entries 6, 7 *vs.* 2). However, the electron delocalization scope of the benzene ring is rather narrow, with the electron-withdrawing effect being more localized. Furthermore, the electron-donating capacity of the benzene ring is relatively feeble, and its offsetting effect on the electron-withdrawing nature of the acyl group is restricted. Consequently, the attenuation of the electron cloud density of the nitrogen atom induced by the acyl group cannot be significantly alleviated. Compared with benzyl ring, the large π system of the anthracene ring can disperse the electron-withdrawing effect of the acyl group more efficiently. Moreover, the strong electron-donating conjugation of the anthracene ring can significantly counteract the electron-withdrawing effect of the acyl group, resulting in a significant reduction in the weakening of the electron cloud density of the nitrogen atom caused by the acyl group (Fig. 4c). As a result, the protonation reaction on the nitrogen atom in anthracene-modified material **2** occurs more readily, leading to higher electrical conductivity than that of material **3** (Table 1, entries 6 *vs.* 7).

In conclusion, an innovative click chemistry strategy to functionalize polyaniline (PANI) with luminescent groups was developed, offering a concise method for preparing luminescent conductive materials. By simply stirring the colloidal dispersion of polyaniline and 9-anthracenecarbonyl chloride solution, luminescent anthracene moieties are efficiently attached to PANI chains *via* amide bonds, which not only preserves the electrical conductivity of PANI but also significantly enhances its fluorescence at specific wavelengths. The large π system of the anthracene ring can efficiently disperse the electron-withdrawing effect of the acyl group, and its strong electron-donating conjugation significantly counteracts the electron-withdrawing effect of the acyl group, resulting in the functionalized material exhibiting a conductivity of 0.232 S/cm after proton doping, >29 times higher than that of the doped PANI. This approach overcomes the drawbacks of traditional methods—namely the interference of functional groups during polymerization and the waste of embedded fluorescent components. It offers a simple and efficient route to luminescent conductive materials, with great potential for fabricating advanced optoelectronic devices without relying on rare metals [35].

CRediT authorship contribution statement

Xiangrong Xu: Writing – original draft, Investigation. **Lifeng Zhang:** Writing – review & editing. **Ming Zhang:** Writing – review & editing. **Yiyang Zhang:** Writing – review & editing, Investigation. **Lei Yu:** Writing – review & editing, Supervision, Funding acquisition, Conceptualization.

Declaration of competing interest

The authors declare that they have no known competing financial interests or personal relationships that could have appeared to influence the work reported in this paper.

Acknowledgments

We thank the Yangzhou Key Research and Development Program: Industry Foresight and Key Core Technology (No. YZ2023019), Cooperation Project of Yangzhou City with Yangzhou University (No. YZ2023209) and Priority Academic Program Development of Jiangsu Higher Education Institutions for support.

Supplementary materials

Supplementary material associated with this article can be found, in the online version, at doi:10.1016/j.cclet.2025.112229.

References

[1] P. Kaushik, R. Bharti, R. Sharma, et al., Eur. Polym. J. 221 (2024) 113574.
[2] S. Li, C.W. Macosko, H.S. White, Science 259 (1993) 957–960.
[3] F. Garnier, R. Hajlaoui, A. Yassar, P. Srivastava, Science 265 (1994) 1684–1686.
[4] Y. Zhou, X. Liu, Z. Wang, et al., Mater. Lett. 308 (2022) 131205.
[5] X. Meng, Y. Zhang, H. Zhou, L. Yu, ACS Sustainable Chem. Eng. 10 (2022) 7658–7663.
[6] S.A. Ture, S.D. Pattathil, V.B. Patil, et al., J. Mater. Sci. Mater. Electron. 33 (2022) 8551–8565.
[7] S.A. Chen, K.R. Chuang, C.I. Chao, H.T. Lee, Synth. Met. 82 (1996) 207–210.
[8] A.C. Anbalagan, J. Korram, P. Koyande, et al., Diamond Relat. Mater. 147 (2024) 111276.
[9] Z. Zeng, Y. Chen, X. Zhu, L. Yu, Chin. Chem. Lett. 34 (2023) 107728.
[10] Z.D. Zhu, Y.Z. Han, X.B. Jing, Rare Met. 43 (2024) 4585–4594.
[11] Y. Zhang, W. Li, Z. Hu, X. Jing, L. Yu, Chin. Chem. Lett. 35 (2024) 108938.
[12] S. Yu, L. Li, Q. Kong, et al., Anal. Bioanal. Chem. 417 (2025) 119–130.
[13] C.S. Cheung, Z. Qiu, D. Li, et al., Dalton Trans. 52 (2023) 17573–17582.
[14] G. Gao, J. Han, L. Yu, Q. Xu, et al., Synlett 30 (2019) 1703–1707.
[15] J. Li, M. Luo, C. Jin, et al., ACS Appl. Mater. Interfaces 14 (2022) 383–389.
[16] I.A. Jessop, F.R. Díaz, C.A. Terraza, et al., Polymers 10 (2018) 553.
[17] K.M. Molapo, A. Venkatanarayanan, C.M. Dolan, et al., Electrochem. Commun. 48 (2014) 95–98.
[18] H.C. Kolb, M.G. Finn, K.B. Sharpless, Angew. Chem. Int. Ed. 40 (2001) 2004–2021.
[19] S.J. Buwalda, Int. J. Biol. Macromol. 282 (2024) 136695.
[20] M. Arslan, A. Degirmenci, R. Sanyal, et al., Polym. Chem. 15 (2024) 4173–4195.
[21] J. Shi, W. Fu, Q. Zou, et al., ACS Appl. Nano Mater. 8 (2025) 10–21.
[22] W. Yu, X. Lu, L. Xiong, et al., Small 20 (2024) 2310799.
[23] S. Wahan, G. Bhargava, P. Chawla, Dyes Pigm. 222 (2024) 111896.
[24] R. Tian, S.M. Xu, Q. Xu, C. Lu, Sci. Adv. 6 (2020) eaaz6107.
[25] F. Chen, X. Lin, Y. Li, et al., Supramol. Mater. 1 (2022) 100003.
[26] Y. Huang, C. Wu, A. Lu, et al., J. Am. Chem. Soc. 147 (2025) 1612–1623.
[27] L. Deng, C. Zhang, B. Li, et al., Chem. Sci. 14 (2023) 3630–3641.
[28] L. Ren, J. Mol. Struct. 1325 (2024) 140951.
[29] W. Li, G. Liu, F. He, S. Hou, Microchim. Acta 191 (2024) 151.
[30] V. Pirota, A. Benassi, F. Doria, Photochem. Photobiol. Sci. 21 (2022) 879–898.
[31] Y. Zhang, L. YU, M. Zhang, Patent, CN202410500501.X, 2024.
[32] X. Zeng, K. Qu, A. Rehman, Acc. Chem. Res. 49 (2016) 1624–1633.
[33] S. Chakraborty, S. Choudhury, N.K. Singha, Small 20 (2024) 2406866.
[34] Y. Wang, A. Liu, T. Li, J. Electron. Mater. 49 (2020) 3751–3760.
[35] Y.H. Ma, X. Gao, W.T. Zhang, et al., Rare Met. 43 (2024) 736–748.